International Journal of Innovative Technology and Exploring Engineering (IJITEE)
ISSN: 2278-3075 (Online), Volume-5 Issue-3, August 2015

Activation of Granulated Blast-Furnace Slag Using Lime Rich Sludge in Presence and Absence of Rice Husk Ash

Saleh Abd El-Aleem Mohamed

Abstract: ***These days there is an increasing emphasis on a cleaner environment and maintaining the balance of the eco-system of the biosphere. It is generally believed that, environmental protection with zero risk and economic growth do not go hand in hand, but at the same time it is also true that, sustainable growth with environmental quality is not an unattainable goal. This work aims at studying the effect of lime rich sludge (LRS) as a byproduct of acetylene industry on the activation of granulated blast-furnace slag (GBFS). LRS was calcined at 850°C for 4h and left to cool in furnace, then slaked with water and dried at 80°C for 24h. GBFS was replaced by 10, 20 and 30 wt., % of LRS. The results showed that, as the amount of LRS increases, the combined water and free lime increase also. The compressive strength values of GBFS-LRS mixes increase with LRS content up to 20 wt., %, and then decrease at 30 wt., % LRS. In order to enhance the compressive strength of the mixture containing 30 wt., % of LRS, different amounts of rice husk ash (RHA) were added. The results indicated that, the compressive strength increases with RHA content. The results of chemical and mechanical properties of GBFS-LRS blends in presences and absence of RHA are in a good agreement with those of XRD, FTIR and TG/DTG analyses.***

Keywords: Granulated blast-furnace slag, Lime rich sludge, Rice husk ash, Compressive strength

I. INTRODUCTION

The creation of waste materials, combined with a growing consumer population has resulted in a waste disposal crisis leading to an economic and environmental problem. These wastes that produced today will remain in the environment for hundreds of years. The magnitude of environmental problems like air, surface and ground water pollution and economic problem like landfilling maintenance cost, etc., is very high for wastes. This rapidly increasing waste stream remains a significant environmental issue and needs to manage in an economic and environmentally sustainable manner. One solution to this crisis lies in recycling waste into useful products to replace the natural/commercial products wherever possible, which will reduce the economic and environmental problem of waste disposal and also reduce the depletion of natural resources **[1]**. Large quantities of sludge are produced across globe and disposed off by landfilling. Space limitations on existing landfill sites have prompted investigations into alternative reuse techniques and disposal routes for sludge. The best practical way of recycling these wastes is to use in civil engineering constructions.

Manuscript published on 30 August 2015.
***Correspondence Author(s)**
Saleh Abd El-Aleem Mohamed, Department of Chemistry, Faculty of Science, Fayoum University, Fayoum, Egypt.

In many countries, the need for locally manufactured building materials can hardly be overemphasized, because there is an imbalance between the demands for housing and expensive conventional building materials coupled with the depletion of traditional building materials. Also, with the expected increase in cement production to meet the need of steadily growing world population and with the urgent need to reduce the amount of energy consumed and CO_2 released in the air, there will be an increasing pressure to reduce cement consumption. To address this situation, attention has been focused on low-cost alternative building materials **[2]**. The use of wastes can contribute to product diversification, decrease final costs, and provide alternative raw materials to several industrial sectors **[3]**. Egypt Government management strategy aims to encourage byproduct disposal by useful reuse according to environmental concepts. Granulated blast-furnace slag (GBFS) is a byproduct formed in the iron manufacture from the fusion of limestone with ash from coke and the siliceous and aluminous residue remaining from the iron ore after the reduction to iron metal. In this process, a molten slag forms as nonmetallic liquid that floats on the top of the molten iron. It is then separated from the liquid metal and cooled. Depending on the cooling mode, three types of slag are produced, i.e., air-cooled slag (ACS), expanded or foamed slag and granulated slag **[4-7]**. The rapid cooling of molten slag by water prevents the formation of large crystals, and the resulting slag normally contains more than 95% of glass (amorphous calcium aluminosilicates). This type of slag is called GBFS or water-cooled slag (WCS) **[8-11]**. Lime rich sludge (LRS), mainly composed of hydrated lime. It is produced as a byproduct of acetylene industry during the exothermic reaction between calcium carbide (CaC_2) and water as the follow:

$$CaC_2 + H_2O \rightarrow C_2H_2 + Ca(OH)_2 + 27 \text{ k. cal.}$$

Lime sludge is generated from paper, acetylene, sugar, fertilizer, sodium chromate and soda ash industries. Approximately 4.5 million tons of sludge in total is generated annually from these industries **[12]**. All the lime sludges other than carbide sludge contain lime as calcium carbonate. The carbide sludge from acetylene industry, mainly contains lime as $Ca(OH)_2$. These sludge essentially contain lime as a major constituent, however, their chemical compositions vary considerably depending upon the composition of limestone used in the parent process. All sludges contain some deleterious constituents/contaminants, e.g. the phospho-chalk from fertilizer industry contains 5-9 percent.

Published By:
Blue Eyes Intelligence Engineering and Sciences Publication (BEIESP)

SO_3, up to 1.5 percent P_2O_5 and up to 2 percent fluoride as major contaminants. Similarly paper, sugar and chromium sludges contain free alkalis up to 2 percent. The chromium and carbide sludges also contain chromium up to 10 percent and chloride up to 2 percent respectively. The presence of these deleterious contaminants restricts their bulk utilization in making cement and related building materials **[13]**. There are few studies on the utilization of lime sludge (LS) to produce cement mortars and concretes. Sahu and Gayathri **[1]** used LS produced from water treatment and fly ash as partial substituents of cement in mortar preparation. Naik **[14]** utilized LS from pulp and paper mills for enhancing strength and durability of ready-mixed concrete. The use of LS with cement for green brick production was also studied in previous research **[15]**. The compressive strength and hydration characteristics of waste paper sludge ash–ground granulated blast-furnace slag (WSA–GGBS) blended pastes were investigated at water to binder (w/b) ratio of 0.5. The strength results are compared to those of normal Portland cement (PC) paste and relative strengths are reported. It was found that, the early relative strengths (1d) of WSA–GGBS pastes were very low but a marked gain in relative strength occurred at 7d and this increased further at 28 and 90 d. For the 50% WSA–50% GGBS blended paste, the strength achieved at 90d was nearly 50% of that of the PC control paste. X-ray diffraction (XRD) and thermo-gravimetric (TG) analysis were carried out to identify the mineral components in the WSA and the hydration products of WSA–GGBS pastes. The principal crystalline components in the WSA are gehlenite, calcium oxide, bredigite and small amounts of anorthite and calcium carbonate and traces of calcium hydroxide and quartz **[16]**. Large quantity of the rice husk (RH) generated in developing countries is normally burnt off in the rice farm/mills or dumped in landfills, while the insignificant portion is used as fuel. Burning in the open air is likely to cause environmental pollution as carbon dioxide (CO_2) and carbon-monoxide (CO) would be released into the atmosphere as a result of insufficient oxygen in the heap of the rice husk. Also, the aerobic decomposition of rice husks in the landfills could be a major source of methane emissions. The release of these gases into the atmosphere changes the climate, thereby resulting in global warming, which is now one of the greatest threats to our world **[17, 18]**. Recycling of the disposed materials is one suitable method of treating the agricultural wastes. When RH is burnt, about 20 wt., % of it is recovered as ash in which more than 75 wt., % is amorphous silica. It is a highly reactive pozzolanic material produced by controlled burning of RH below 800ºC **[19-21]**. The RHA is a byproduct of paddy industry and it is hazardous to environment if not disposes properly **[22, 23]**. Unlike natural pozzlolana, RHA is an annually renewable source of silica. According to ASTM **[24]**, after chemical analysis of a given material if the sum of Iron oxide (Fe_2O_3), Silicon oxide (SiO_2) and Aluminum oxide (Al_2O_3) is more than 70%, then the material would be declared as a pozzolanic material. RHA is used to produce cement concrete with improved workability, low heat of hydration, reduced permeability, and enhanced strength **[25-29]**. In this paper, the impact of lime rich sludge (LRS), as a byproduct of acetylene industry on the hydration of GBFS was estimated. Also, the hydration characteristics of GBFS/LRS blends in presence and absence of RHA were studied.

II. MATERIALS AND EXPERIMENTAL TECHNIQUES

II. (A). MATERIALS

The materials used in this investigation were lime rich sludge (LRS), granulated blast-furnace slag (GBFS), and rice husk ash (RHA). LRS was provided from INSOMAT Company, Tammoh, Giza Governorate, Egypt, GBFS was supplied from Iron and Steel Company, Helwan, Egypt. GBFS was mechanically ground to Blaine surface area of 3500 cm^2/g. Rice husk (RH) was collected from paddy field in Tatoon, Etsa, El-Fayoum, Egypt. It was purified by boiling for 1h to remove of pentosane and lignin, and then the sample was washed with distilled water and dried at 110ºC for 24h. The dried RH with grain size 0.5 mm was burnt at 450ºC, RHA with more than 90% silica content and surface area of 60 m^2/g was obtained. The amorphous characters of BFS and RHA are confirmed by X-ray diffraction as shown in Fig.1. The oxide analyses of GBFS, LRS and RHA obtained by X-ray fluorescence (XRF) spectrometry are given in Table 1.

II. (B). EXPERIMENTAL TECHNIQUES

Firstly, lime rich sludge (LRS) was calcined at 850ºC for 4h to remove any hydrated and carbonated materials. It was cooled in the furnace and slaked with water to form hydrated lime, and then dried in an oven electric drier at 80ºC for 24h. The dry LRS was kept in a desiccator to avoid atmospheric moisture and carbonation. It was pulverized to a fixed particle size of 45µm. GBFS was replaced by LRS with 10, 20 and 30 wt. %. In order to determine the pozzolanic activity of RHA, different RHA percentages (5, 7.5 and 10 wt., %) were added to GBFS-LRS blend, containing 30 wt., % of LRS as shown in Table 2. The ingredients of each dry mixture (BFS-LRS or BFS-LRS-RHA) were blended in a porcelain ball mill for 1h using a mechanical roller mill to ensure complete homogeneity. The dry samples were placed on smooth, non-absorbent surface, and then mixed with water at water to cement (W/C) ratio of 0.25 and a crater was formed in the center, then water was poured into the crater. The dry portion of mixture was slightly toweled over the remaining mixture to absorb the water for about 1min. The mixing operation was then completed by continuous and vigorous mixing using ordinary gauging trowel for about 3 minutes. The pastes were manually placed, pressed and homogenized in one inch stainless steel cubic molds. The molds were vibrated for few minutes for better compaction. After the top layer was compacted, the top surface of the mold was smoothened by the aid of thin edged trowel. The specimens were cured for 24h in humidity chamber with 100% RH, then demoded and cured under tap water for further investigations at different curing times (1, 28 and 90 days). After the predetermined curing time, the hydration of cement pastes were stopped by pulverizing 10g of representative sample in a beaker containing 1:1 methanol–acetone mixture, then mechanically stirred for 1h.

Published By:
Blue Eyes Intelligence Engineering and Sciences Publication (BEIESP)

The mixture was filtered through a G4, after washing several times with the stopping solution and diethyl ether, then dried at 70ºC for 1h, then collected in polyethylene bags; sealed and stored in desiccators for further analysis **[30]**. The chemically combined water content is considered as the percent of ignition loss of the dried sample (on the ignited weight basis). Approximately 2g of the predried sample were ignited up to 1000ºC for 1h soaking time. The results of combined water contents were corrected for the water of free lime present in each sample **[10, 31]**. The free lime content of each hydrated cement paste was estimated by the following method, the sample (0.5 g) was poured in 40 ml of a glycerol-ethanol mixture (1:5 v/v), together with a small amount of anhydrous $BaCl_2$ (0.5g) as a catalyst, and phenolphthalein as an indicator. This mixture was kept in a conical flask, fitted with an air reflux, heated on a hot plate for 30 minutes (the color becomes pink). The contents of the flask were titrated with a standardized (0.1N) alcoholic ammonium acetate solution until the pink color just disappeared. Heating was again affected, and if the pink color reappears, the titration was completed with ammonium acetate solution until no further appearance of pink color occurs up on heating. CaO, % = [(W1×V)/W] ×100, W = original weight, W1 = weight of CaO equivalent to amount of added alcoholic ammonium acetate, V = volume of ammonium acetate per ml **[32]**. At each time of testing, the compressive strength was measured according to ASTM C109M-12 **[33]**. A set of three cubes were dried in an oven drier at 105ºC for 24h. The compressive strength measurements were done on a compressive strength machine of Seidner, Riedinger, Germany, with maximum capacity of 600 KN force. To verify the mechanism predicted by the chemical and mechanical tests, some selected hydration products were investigated using XRD, FTIR, TG and DSC techniques. The powder method of XRD was adopted in the present study. For this, a Philips diffractometer PW3050/60 with X-ray source of Cu kα radiation (λ=1.5418Å) was used. The scan step size was 2θ. The collection time 1s, and in the range of 2θ from 5 to 60º. The X-ray tube voltage and current were fixed at 40.0 KV and 40.0 mA respectively. An on-line search of a standard database (JCPDS database) for X-ray powder diffraction pattern enables phase identification for a large variety of crystalline phases in a sample **[34]**. The DTA was carried out by heating the sample in nitrogen atmosphere up to 1000°C using a DT-30 Thermal Analyzer (Schimadzu Co-Kyoto, Japan). Calcined alumina was used as inert material, about 50 mg (76µm) of each. The finely ground hydrated cement paste were housed in a small platinum-rhodium crucible. A uniform heating rate was adopted in all of the experiments at 20ºC/min **[34]**. The infrared (IR) spectral analysis was recorded using alkali halide pressed disk technique as it gives a further reduction in scattering **[35]**. Exactly 2.0 mg of the sample was ground with 198 mg of potassium bromide in agate mortar to produce a homogeneous mixture. The mixture was pressed under vacuum to give a transparent disk of 1 cm in diameter. The infrared spectral analysis was recorded from KBr disks using Mattson Gensis IR in the range of 400-4000 cm^{-1}.

III. RESULTS AND DISCUSSION

III (A). Chemically combined water

Fig. 2(a) shows the variation of Wn %, of hydrated GL10, GL20 and GL30 blends at different curing times. It is clear that, the Wn, % values increase sharply with the hydration time up to 28 day; this is due to the direct contact between water and the solid grains of BFS/LRS mix and accumulation of hydrated products in some of open pores; leading to the increase in Wn, %. But, at 90 days, the Wn increases gradually; this is due to the decrease in the rate of diffusion of water through the coating of hydration products into the unhydrated parts of BFS and LRS grains. Obviously, at all curing ages, the Wn, % of hardened pastes made of GL30 are higher than those of GL10 or GL20 mixes. This is ascribed to the high lime content in the hardened paste of GL30. Fig. 2(b) represents the Wn contents of hardened BFS-LRS pastes (GL30) containing 5 (GL30R5), 7.5 (GL30R7.5) and 10 wt., % (GL30R10) of RHA at different curing times. It can be seen that, Wn contents of hardened paste made of GL30R10 mix shows the lowest value at one day of curing. This is attributed to that, the active silica of RHA retards the hydration rate of GBFS-LRS pastes at early age as a result of the formation of silica gel. On the other hand, the higher the RHA content, the higher the combined water values at later age of hydration. This fact should be due to that, the active silica in RHA reacts with free lime to form additional CSH with high combined water content. The Wn value of GL30R10 mix is closed and nearly the same value to that of GL30R7.5 at 28 days of hydration. This proves that, the most of free lime content is consumed by the addition of 7.5 wt. % RHA.

III (B). Free lime content

Fig. 3(a) shows the free lime values of hydrated GL10, GL20 and GL30 mixes at different curing times. It is evident that, for all mixes the free lime contents (FL, %) decrease with curing time. This is attributed to the continuous pozzolanic reaction between LRS and BFS with the formation of calcium silicate hydrate (CSH) and calcium alumino-silicate hydrate (CASH). On the other side, the values of free lime content of M10 are lower than that of M20 or M30. This is evident that, the free lime increases with LRS content in BFS-LRS blends. The Pozzolanic reaction rate of RHA with the liberated lime during the hydration of GBFS-LRS-RHA mixes can be followed by monitoring the decrease in FL, % with curing time and RHA, %. Fig. 3(b) represents the variation in free lime contents of GL30, GL30R5, GL30R7.5 and GL30R10 at different curing times. Obviously, the free lime contents decrease with the increase of RHA%, suggesting that, the active silica in RHA reacts with free lime to form CSH. Furthermore, the amount of CSH increases on the expense of FL as shown later in TGA/DTG and XRD analyses. The free lime contents of GL30R10 are nearly the same to those of GL30R7.5 at later ages of hydration, indicating that, the most amount of FL is consumed by the addition of 7.5 wt., % RHA. The results of free lime contents for all mixes are in accordance with those of combined water.

Published By:
Blue Eyes Intelligence Engineering
and Sciences Publication (BEIESP)

III (C). Compressive strength

Fig. 4(a) shows the compressive strength values of hydrated GL10, GL20 and GL30 mixes at different curing times. It is clear that, the compressive strength values of all hardened specimens increase with hydration time up to 90 days. This is ascribed to the continuous formation of CSH on prolonged hydration of BFS/LRS pastes; these hydrates act as binding centers of the remaining unhydrated residual parts of GBFS. Evidently, the compressive strength values increase with LRS content up to 20 wt.,% (GL20), then decrease when the blend contains 30 wt.,% of LRS (GL30). This is attributed to that, the activation or dissolution of GBFS enhances with the increase of LRS content up to 20 wt.,%, leading to increase the compressive strength; meanwhile, there is excess lime content does not react with GBFS in case of GL30, leading to the increase of free lime content, which negatively affects the mechanical properties of hardened paste. In addition, the formed CSH seems to possess higher lime content for the paste made of mix GL30 as compared to the CSH of the paste made of GL20 or GL10 mixes, which have lower lime content; lime-rich CSH possess lower hydraulic properties than those of lime-poor CSH. Fig. 4(b) represents the compressive strength values of GL30, GL30R5, GL30R7.5 and GL30R10 at different curing times. Comparing compressive strength values of samples with and without RHA, we find that, the RHA negatively affects the compressive strength of samples at early hydration ages, especially at 1 day followed by observable increasing in compressive strength value beginning from 28 days. The compressive strength value of mix containing 7.5 % RHA is higher than that of the mix containing no RHA by ~ 63 % after 90 days of hydration. Besides, the more addition of RHA (10%) has a marginal effect on the compressive strength gain of the hardened samples. These are due to that, the addition of 7.5% RHA is favor to the consumption of free lime in GL30, forming additional amount of CSH, which responsible for the increase in strength properties.

III (D). XRD analysis

Fig. 5(a) represents XRD patterns of GL20 at 1, 28 and 90 days of hydration. Generally, the XRD diffractograms show different peaks related to calcium hydroxide (CH), calcium silicate hydrate (CSH), and calcium carbonate (CC). The results show that, the intensity of characteristic peaks for CSH and CC increase with time on the expense of the CH peak intensity. This seems to be due to the continuous activation of GBFS by CH, present in LRS to form CSH. Moreover, with curing time, some of CH is atmospherically carbonated. Fig. 5(b) shows the XRD diffractograms of hydrated samples made of GL10, GL20 and GL30 at 90 days of curing. It is clear that, have shown that, the M30 mix has the highest amount of remained CH as compared with mixes GL20 or GL10. This is in a good harmony with the results of free lime. In addition, the peak corresponding to CSH of GL20 is more intense than that of GL10 or GL30. This demonstrates that, the mix containing 20% LRS presents the highest compressive strength than the other investigated mixes. Besides, the GL10 mix has low amount of CH, which not sufficient for the complete GBFS-dissolution. Conversely, the mix GL30 contains high amount of LRS, which causes the complete dissolution of GBFS in the mix. The GL20 mix has the suitable amount of LRS required for the activation and dissolution of GBFS, and therefore, the formation of excess amounts of hydration products. The XRD-results are in a good agreement with those of compressive strength. Fig.5 (c) shows XRD patterns of hardened pastes made of GL30, GL30R5, GL30R7.5 and GL30R10 at 90 days of hydration. Generally, all patterns exhibit the same characteristic peaks of CSH, CH and CC, but they differ in the degree of peak intensity. The CH peak intensity decreases with the increase of RHA percentages from 5 up to 10%. Also, the CC and CH peak intensities of all samples containing RHA are lower than those of the samples free from RHA. This can be explained by free CH consumption through the high pozzolanic interaction with RHA, leading to the formation of additional CSH. Furthermore, the presence of RHA in the system decreases the probability of atmospheric carbonation. The presence of 10% RHA shows a marginal effect on the CH-consumption in the sample matrix as compared with 7.5%

III (E). FTIR spectroscopy

Fig.6 (a) displays the FTIR-spectra of GL20 at 1, 28 and 90 days of hydration. The absorption band at 476 cm-1 is related to the O–Si–O bending vibration. The short absorption bands at 689 and 715 cm^{-1} are assigned to the symmetric stretching vibrations of the Si–O–Al. The absorption bands at 876, 1459-1492 cm^{-1} are related to the carbonate containing phases. The strong absorption band located at 969-991 cm^{-1} corresponds to the asymmetric stretching vibration of Si-O-T (T: Si or Al). The absorption bands at 1665-1661 cm^{-1} correspond to the bending vibration of H-OH, while the absorption band at 3439-3548 cm^{-1} is related to the symmetric stretching vibration of OH group. The intensity of this band decreases with curing time. This seems to be due to the consumption of LRS as a result of GBFS activation with time, forming more hydration products, which can be observed from the increase of absorption band intensity related to Si-O-T with curing time. Besides, the high full width at half maximum (FWHM) of this band decreases with time. Also, this band shifts to low wavenumber with the increase of curing time up to 90 days. Both the shift to low wavenumber and the decrease in FWHM are related to the increase in CSH crystallinity, which caused by the structure ordering of silicate network. On the other hand, the intensity of absorption band related to atmospheric carbonation increases with time, suggesting the continuous carbonation of hydrated lime with curing time. Fig. 6(b) shows the FTIR-spectra of the hardened pastes of GL10, GL20 and GL30 at 90 days of curing. It can be observed that, the absorption bands related to atmospheric carbonation at 876 and 1489-1496 cm^{-1} of GL30 are more intense than those of GL20 or GL10. This is due to the relatively high free lime content of GL30. FWHM of well resolved absorption band corresponds to Si-O-T at 967 cm^{-1} of GL20 is smaller than that of GL10 or GL30, indicating the high structure ordering of silicate network formed in GL20.

Published By:
Blue Eyes Intelligence Engineering and Sciences Publication (BEIESP)

Fig. 6 (c) illustrates the FTIR spectra of GL30, GL30R5, GL30R7.5 and GL30R10 at 90 days of hydration. The intensities of the absorption bands related to H-O-H stretching vibration and OH bending vibration at 1648-1659 cm^{-1} and 3534-3584 cm^{-1} decrease with RHA content. This proves that, the free lime consumption increases with RHA percentage. The GL30R10 shows the lowest carbonation comparing to the all other investigated mixes (GL30, GL30R5 and GL30R7.5). This is in a good agreement with the results of XRD analysis.

III (F). TG/DTG analysis

Fig.7 (a & b) respectively represents TGA and DTG thermograms of hydrated GL20 at 1, 28 and 90 days, respectively. The weight losses of hydration products were determined from the TGA plots (Fig.7a). It is apparent that, the weight loss at 1000°C of GL20 increases with curing time from 1 up to 90 days. This is attributed to the continuous activation and dissolution of GGBFS portion, leading to the formation and accumulation of additional amount of CSH, which results in the increase of the CSH peak intensity at 50-200°C as shown in the DTG thermograms (Fig. 7b). It can be seen that, the endothermic peak related to calcium hydroxide (CH) at 481°C declines with the increase of curing time. This is due to the reaction of CH present in LRS with GBFS, resulting in the formation of CSH and CASH, therefore, the intensity of CSH endothermic peak increases on the expense of CH peak with hydration age. The intensity of endothermic peak related to calcium carbonate increases with time. This is ascribed to the increase of the CH-atmospheric carbonation with curing time. Fig. 8 (a & b) respectively shows the TG/DTG thermograms of hardened pastes made of GL10, GL20 and GL30 mixes at 90 days. Obviously, the weight loss of hardened paste made of GL30 is greater than that of GL10 or GL20. This is due to the relatively high amounts of CH and CC in hardened paste of GL30 as compared to those of GL10 or GL20 as shown in DTG thermograms (Fig. 8 b). Clearly, the amount of CSH formed in GL20 is higher than that in GL10, indicating that, the degree of pozzlolanic activity increases with the LRS content. Conversely, the amount of CSH formed in GL30 is nearly the same of that formed in GL20, suggesting that, the 20% LRS is sufficient for the activation of GBFS-hydration. Fig. 9 (a & b) respectively represents TG/DTG thermograms of hardened pastes with no RHA (GL30) and with 5(GL30R5), 7.5 (GL30R7.5) as well as 10% (GL30R10) of RHA at 90 days of hydration. It is shown that, the amount of CH decreases with the increase of RHA content, suggesting that, the RHA reacts with free lime, forming additional CSH. In parallel, the amount of calcium carbonate decreases with RHA content. This proves that, the free lime consumption as a result of RHA addition. The amount of CSH increases sharply with RHA up to 7.5%, and then slightly at 10% RHA.

IV. CONCLUSIONS

From this study the following conclusion can be drawn:

1-As the amount of LRS increases the chemically combined water and free lime contents increases.

2-The compressive strengths of GBFS-LRS mixes increase with the amount of LRS up to 20%, and then decrease at 30% of LRS.

3-The higher the amount of RHA, the lower the combined water at one day of curing. Meanwhile, at later hydration ages, the combined water contents increase with RHA percentage. In contrast, the free lime contents decrease with the increase of RHA, % at all ages of curing. The combined water and free lime contents as well as compressive strength values of GBFS-LRS mix containing 10% RHA are nearly the same and closed to the corresponding values of GBFS-LRS mix containing 7.5% RHA, indicating that, the addition of 7.5% RHA to GBFS-LRS is the optimum addition level.

4-The RHA has a good pozzolanic activity as confirmed by the decrease in free lime content and the decrease in the intensity of CH characteristic peaks in XRD, FTIR and DSC techniques as well as the increase of the compressive strength values with RHA content.

5-The GBFS-LRS-RHA composite, which contains 30% LRS and 7.5% RHA can be beneficially used to prepare low cost temporary structure. It can be used in preparation of non-structural elements in the low range compressive strength where strength is not required. Also, this composite may be used in masonry mortar to improve the long-term strength.

REFERENCES

1. Sahu V., Gayathri V., “The Use of Fly Ash and Lime Sludge as Partial Replacement of Cement in Mortar”, Intern. J. of Eng. Tech. Innov., 4(1), (2014), pp. 30-37.
2. Kumar R., “Effect of partial replacement of cement by fly ash and lime sludge on strength characteristics of concrete”, A thesis of Master of Engineering in Structural Engineering (ROLL NO.821022004), Department of Civil Engineering, Thapar University, Patiala 147004 December, (2013).
3. Menezes RR., Ferreira HS., Neves GA., Lira LRS., Ferreira HC., “Use of granite sawing wastes in the production of ceramic bricks and tiles”, J. Eur. Ceram. Soc.; 25(2005), pp. 1149–58.
4. Li C., Sun H., Li L., “A review: the comparison between alkali activated slag (Si+Ca) and metakaoline (Si+Al) cements”, Cem. Concr. Res. 40 (2010), pp 1341–1349.
5. Chen W., “Hydration of slag cement: theory, modeling and application”, PhD Thesis, University of Twenty; (2007).
6. Sabrah B. A., Abd El-Aleem S., Gouda H., “Physico-mechanical and Chemical Properties of Composite Cement Containing High Percentages of Mechanically Activated Egyptian Slag”, International Journal of Engineering Research & Technology (IJERT); 3(9) (2014), pp. 1446-1457.
7. Abd El-Aziz Abdel Gawwad H., Mohamed Khater H., Abd El-Aleem Mohamed S., “Impact of Alkali Concentration and Metakaolin Content on Accelerated Ageing of Egyptian Slag”, American Journal of Chemical Engineering; 3(3) (2015), pp. 30-38.
8. Abd El-Aleem S., "Hydration characteristics of granulated slag with fired by-pass cement dust", Sil. Ind; 69 (3-4); (2004), pp. 46-52.
9. Heikal M., Abd El-Aleem S., and Morsi W.M., “Characteristics of blended cements containing nano-silica” HBRC Journal (9) (2013), pp. 243–255.
10. Abd-El.Aziz M.A., Abd.El.Aleem S., and Heikal M., “Physico-chemical and mechanical characteristics of pozzolanic cement pastes and mortars hydrated at different curing temperatures” Constr. Build. Mater. 26; (2012), pp. 310–316.
11. Siddique R., “Waste Materials and By-Products in Concrete”, Springer-Verlag. Berlin (Heidelberg), (2008).
12. Calkins, R. J., Novak J. T., “Characterization of Chemical Sludges,” Journal of American Water Works Association, 65 (6) (1973), p. 423.

Published By:
Blue Eyes Intelligence Engineering and Sciences Publication (BEIESP)

13. CPCB, “Assessment of Utilization of Industrial Solid Wastes in Cement Manufacturing”, Central Pollution Control Board, New Delhi, (2007).
14. Naik, T. R., “Use of Residual Solids from Pulp and Paper Mills for Enhancing Strength and Durability of Ready-Mixed Concrete”, (2002).
15. Nafsal k., Ramasamy T., “The Use of Lime Sludge and cement for the Production of Green Brick”, International Journal on Applications in Civil and Environmental Engineering, 1(1), (2015), pp. 6-8.
16. Bai J., Chaipanich A, Kinuthia J.M, O'Farrell M., Sabir B.B., Wild S., Lewis, “Compressive strength and hydration of wastepap M.H er sludge ash–ground granulated blastfurnace slag blended pastes”, Cem. Concr. Res., 33, 8, August (2003), pp. 1189-1202.
17. James S. Fabiyi, “Suitability of Portland Cement and Rice Husk Ash Pozzolan Systems for Cement Bonded Composites Production”, J. Mater. Environ. Sci. 4 (6) (2013), pp. 848-854.
18. Habeeb G. A, Bin Mahmud H., “Study on Properties of Rice Husk Ash and Its Use as Cement Replacement Material”, Materials Research; 13(2), (2010), pp. 185-190.
19. Kartini. K, “Rice Husk Ash pozzolanic material for sustainability—Universiti Teknologi MARA 40450 Shah Alam,

Published By:
Blue Eyes Intelligence Engineering
and Sciences Publication (BEIESP)

Selangor Malaysia", International Journal of Applied Science and Technology Vol. 1 No. 6; November, (2011).
[20] Heikal M., Abd El.Aziz M., Abd El.Aleem S., El. Didamony H., "Effect of polycarboxylate on rice husk ash pozzolanic cement", Silicates Industriels; 69 (9-10) (2004), pp. 73-84.
[21] Nair D., Fraaij A., Klaassen A. and Kentgens A. A, "structural investigation relating to the pozzolanic activity of rice husk ashes", Cement and Concrete Research (Elmsford), 2008; 38(6):861-869.
[22] Muthadhi A., Anitha R., Kothandaraman S, "Rice Husk Ash Properties and its uses: A Review", Journal CV Vol 88, May (2007).
[23] Naji Givi A., Abdul Rashid S. , Nora A. Aziz F., Amran Mohd Salleh M., "Contribution of Rice Husk Ash to the Properties of Mortar and Concrete: A Review", Journal of American Science; 6 (3) (2010).
[24] Specification for Fly Ash and Raw or Calcium Natural Pozzolona for Use as a Material Admixture in Portland Cement Concrete, ASTM C 618-78, American Standard for Testing Materials, (1978).
[25] Mehta P.K., "Siliceous ashes and hydraulic cements prepared therefrom", US Patent, 4105459 A, August, (1978).
[26] Abu Bakar B. H.; Ramadhansyah P. J., Megat Azmi M. J., "Effect of rice husk ash fineness on the chemical and physical properties of concrete", Magazine of Concrete Research, 63 (5), (2011), pp. 313 – 320.
[27] Khassaf S. I., Jasim A. T., Mahdi F.K., "Investigation The Properties Of Concrete Containing Rice Husk Ash To Reduction The Seepage In Canals", International Journal of Scientific& Technology Research, 3(4), (2014), pp. 348-354.
[28] Talsania S., Pitroda J., Vyas C.M., "Effect of rice husk ash on properties of pervious concrete", Int. J. Adv. Eng. Res. Studies/IV/II/Jan.-March, (2015), pp. 296-299.
[29] Maurice et al., "Compressive strength of concrete with rice husk ash as partial replacement of ordinary Portland cement", Department of Civil Engineering, Rivers State University of Science and Technology Port Harcourt, Nigeria, Scholarly Journal of Engineering Research, 1(2) (2012), pp. 32-36.
[30] Abd El-Aleem Mohamed S., Mohamed Morsi W., "Performance of Nano–Modified Cement Pastes and Mortars in Caron's Lake Water", International Journal of Engineering and Advanced Technology (IJEAT), Volume-4 Issue-6, August (2015), pp. 80–94
[31] El-Didamony H., Abd-El. Eziz M., and Abd.El.Aleem S., "Hydration and durability of sulfate resisting and slag cement blends in Qaron's Lake water", Cem. Concr. Res., 35; (2005), pp. 1592-1600.
[32] Abd El-Aleem Mohamed S., El-Rahman Ragab A., "Physico-Mechanical Properties and Microstructure of Blended Cement Incorporating Nano-Silica", International Journal of Engineering Research & Technology (IJERT), Vol. 3 Issue 7, July (2014), pp. 339-358
[33] ASTM C109M, "Standard test method for compressive strength of hydraulic cement mortars", (2012).
[34] Ramachandran V.S., "Thermal Analysis, in; Handbook of analytical techniques in concrete science and technology" , Ramachandran V.S. and Beaudoin J. J. Eds., Noyes publications, New Jersey. ISBN: 0-8155; (2001), PP.1473-1479.
[35] Errington RJ., "Advanced practical inorganic and metalorganic chemistry", Blackie Academic & Professional, An Imprint Chapman & Hall: (1997).

Table 1: Chemical compositions of GBFS, LRS and RHA, wt. %

Oxide,%	SiO_2	Al_2O_3	Fe_2O_3	CaO	MgO	Na_2O	K_2O	SO_3	TiO_2	P_2O_5	L.O.I	Total
GGBFS	43.71	9.78	0.62	35.92	5.43	0.89	0.61	1.29	0.35	0.17	1.20	99.97
LRS	2.23	0.81	0.24	90.00	0.08	0.23	0.21	0.38	0.16	----	5.64	99.98
RHA	91.42	2.19	0.48	1.53	0.64	0.17	1.33	----	-----	1.14	1.05	99.95

Table 2: Mix composition of the prepared samples

Mix. Symbol.	BFS, wt. %	LRS wt., %	RHA wt., %
GL10	90	10	0
GL20	80	20	0
GL30	70	30	0
GL30R5	70	30	5
GL30R7.5	70	30	7.5
GL30R10	70	30	10

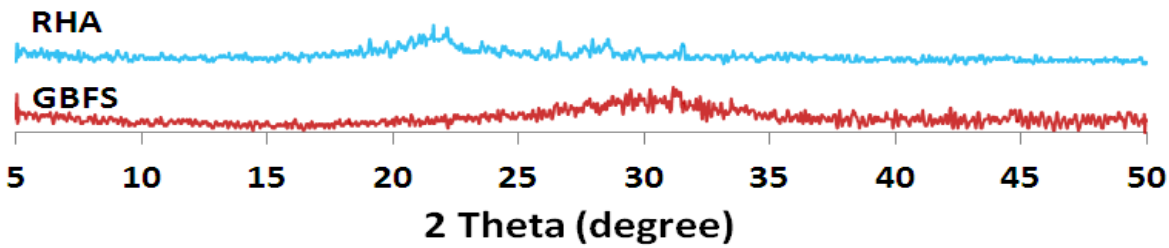

Fig. 1. XRD pattern of GBFS and RHA

Published By:
Blue Eyes Intelligence Engineering
and Sciences Publication (BEIESP)

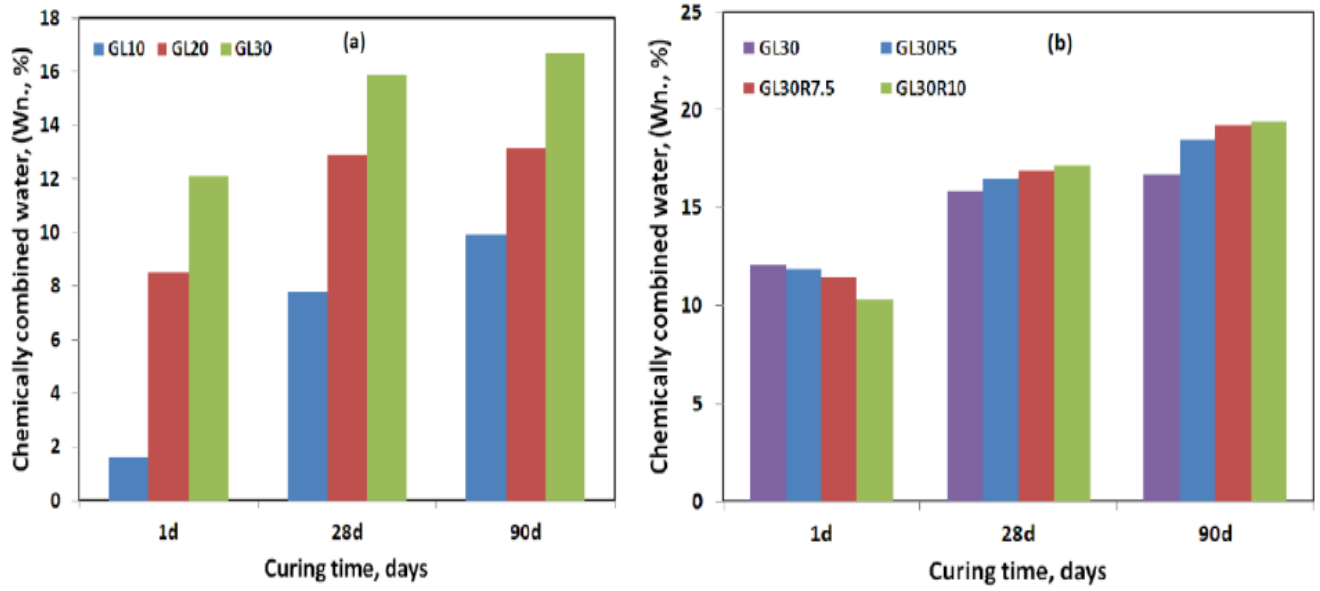

Fig. 2 (a) Combined water of GBFS-LRS and (b) GBFS-LRS-RHA mixes at different curing times

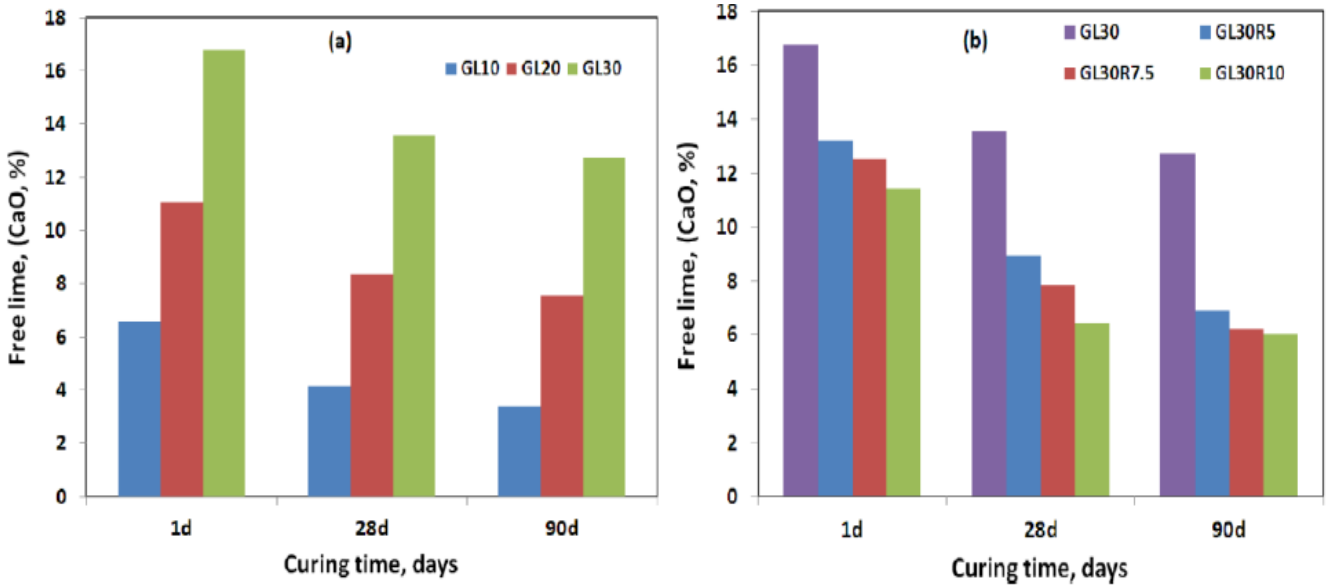

Fig. 3. (a) Free lime of GBFS-LRS and (b) GBFS-LRS-RHA mixes at different curing times

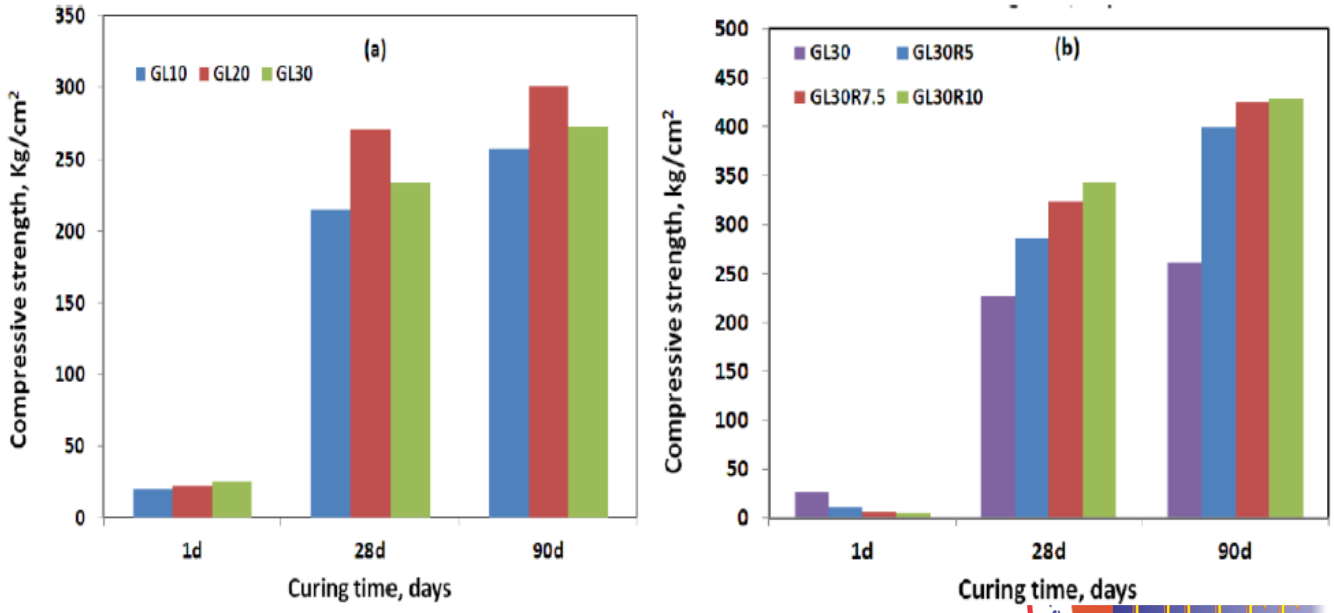

Published By:
Blue Eyes Intelligence Engineering
and Sciences Publication (BEIESP)

Fig. 4. (a) Compressive strength of BFS-LRS and (b) BFS-LRS-RHA mixes at different curing times

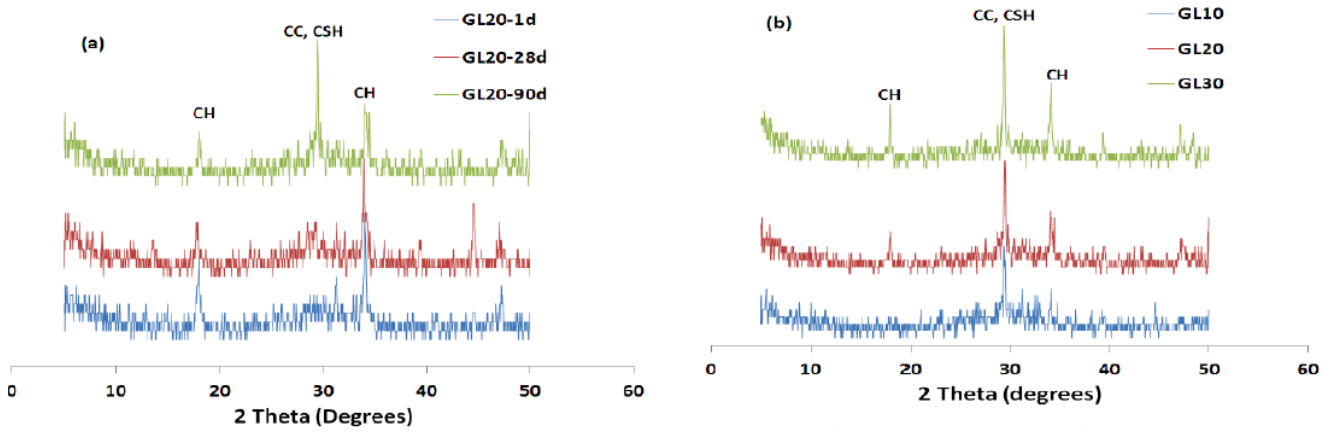

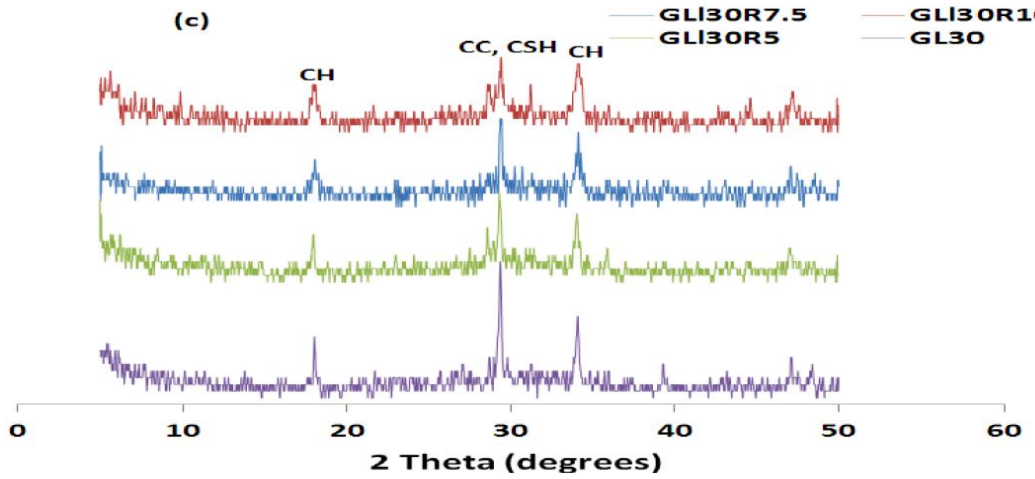

Fig. 5. XRD diffract grams of (a) GL20 at 1, 28 and 90 days, (b) GL10, GL20 and GL30 at 90 days and (c) GL30R5, GL30R7.5 and GL30R10 at 90 days

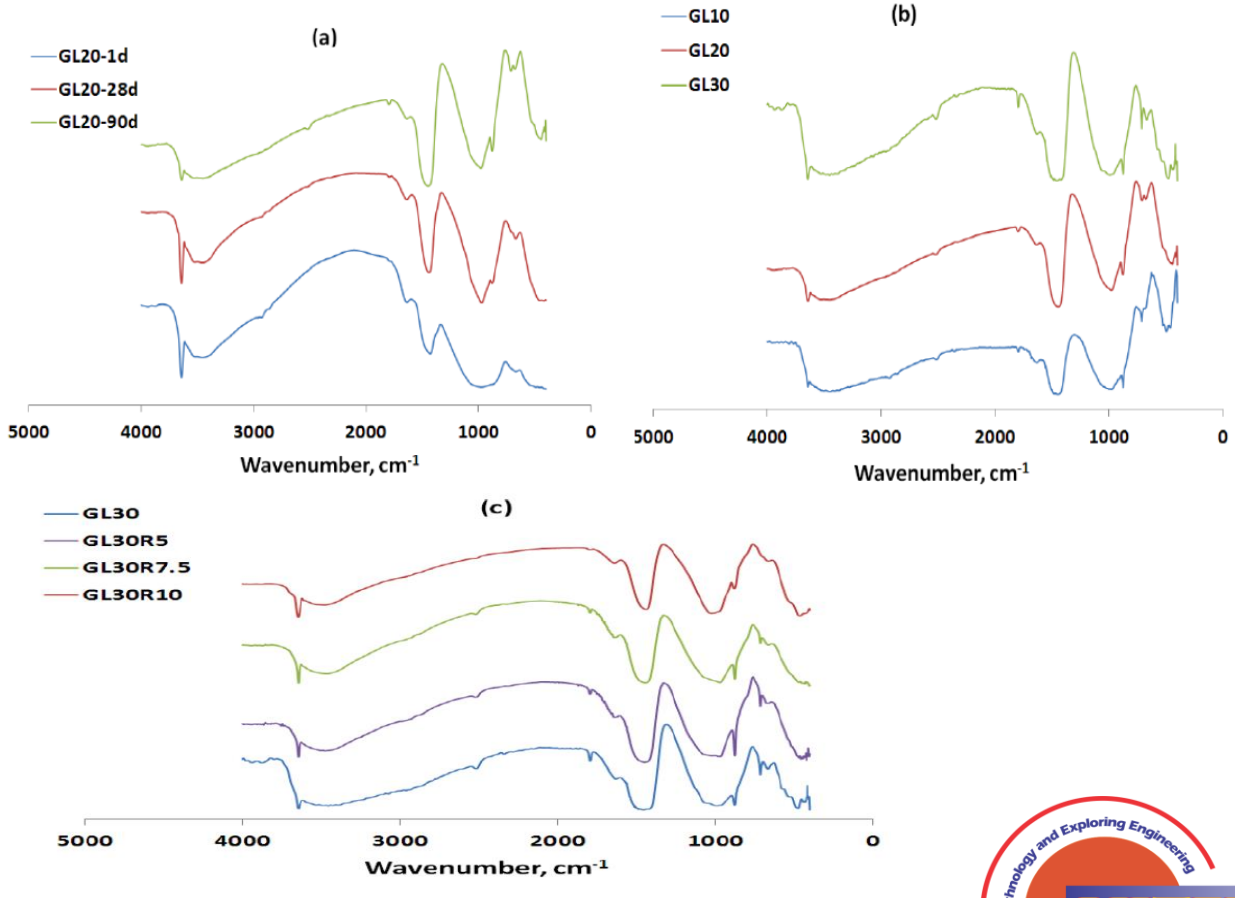

Published By:
Blue Eyes Intelligence Engineering
and Sciences Publication (BEIESP)

Fig. 6. FTIR spectra of (a) GL20 at 1, 28 and 90 days, (b) GL10, GL20 and GL30 at 90 days and (c) GL30R5, GL30R7.5 and GL30R10 at 90 days

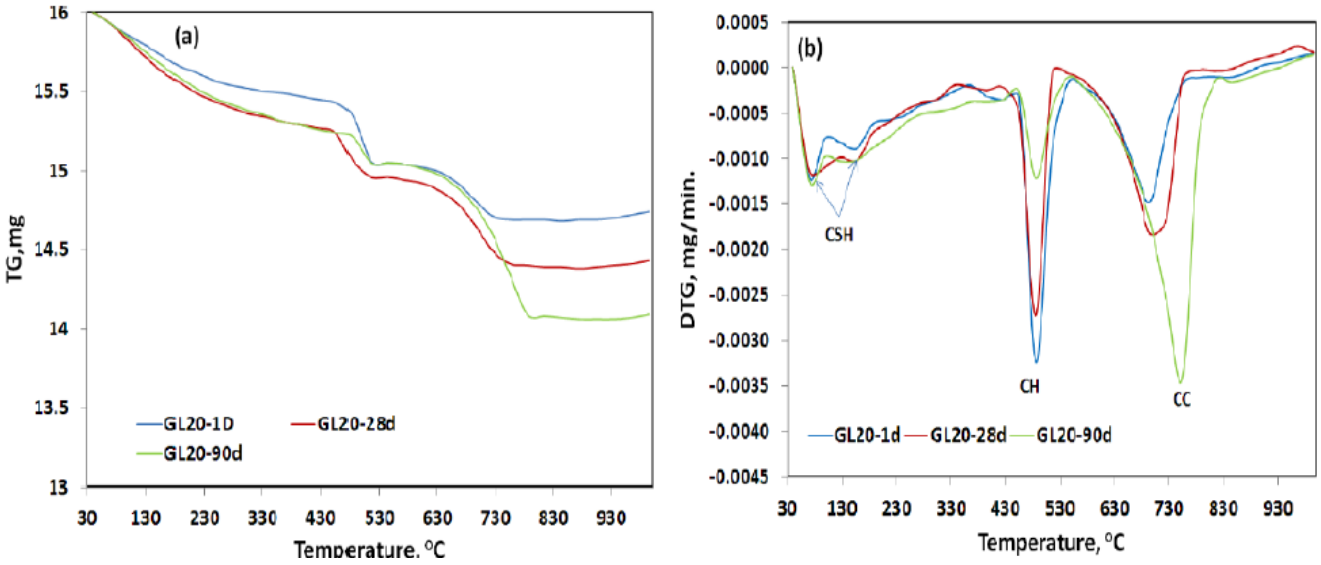

Fig. 7. (a) TG and (b) DTA-Thermograms of hydrated GL20 pastes at 1, 28 and 90 days

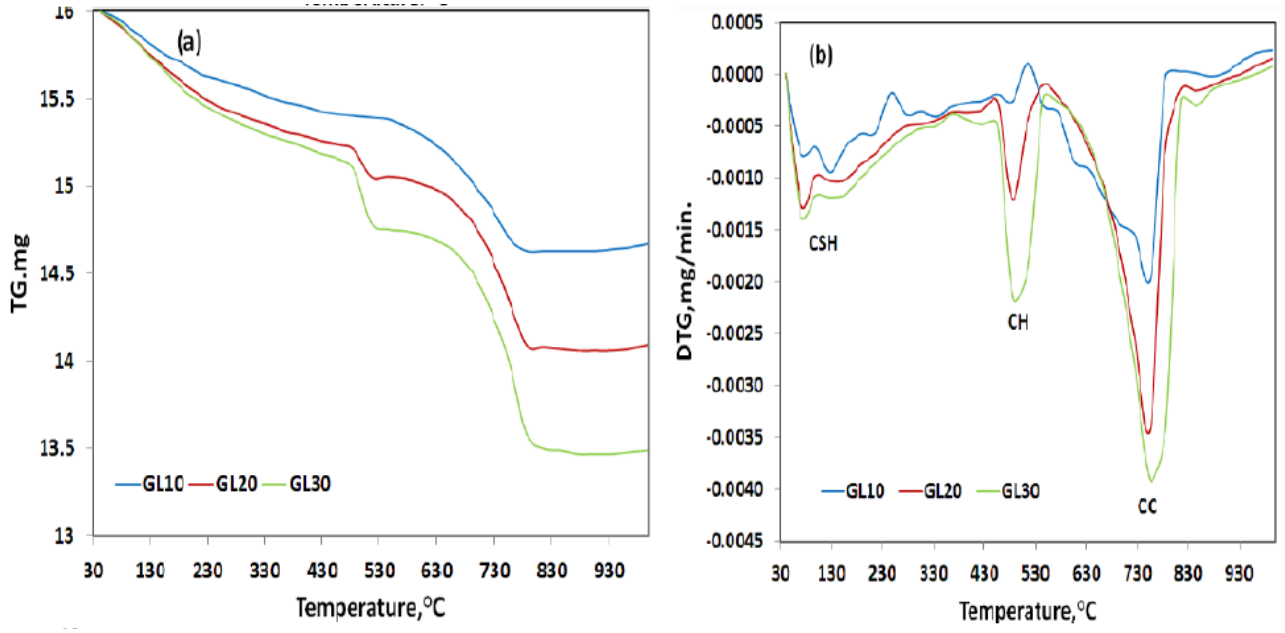

Fig. 8. (a) TG and (b) DTA-Thermograms of hydrated GL10, GL20 and GL30 at 90 days

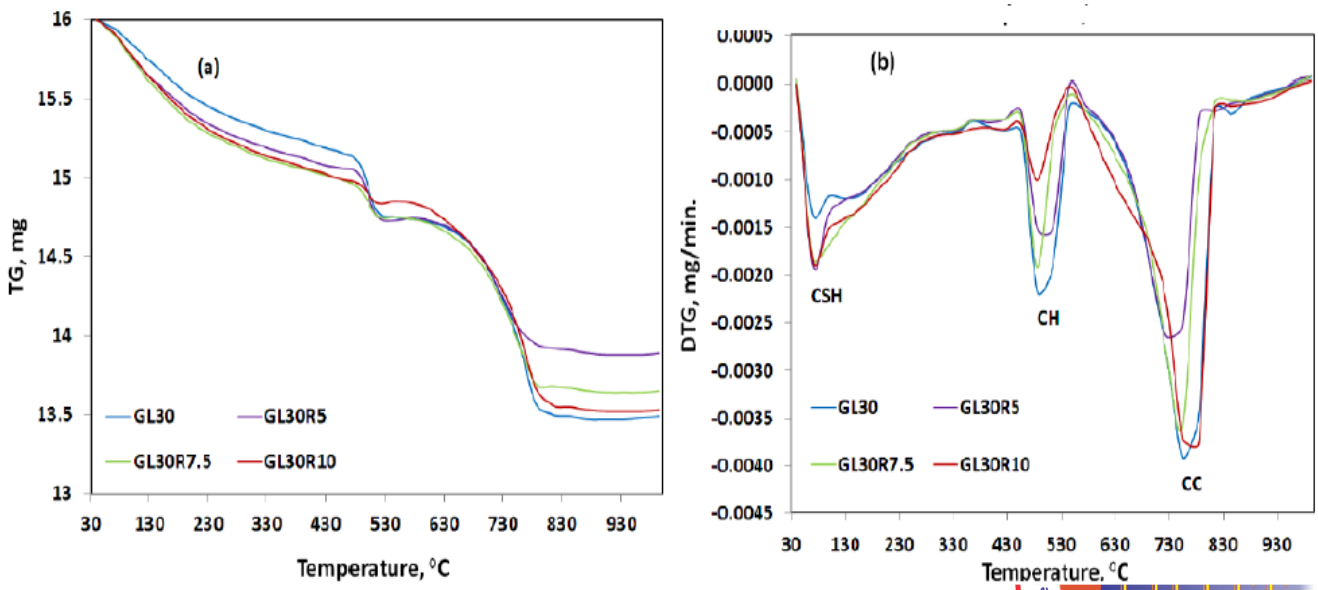

Published By:
Blue Eyes Intelligence Engineering
and Sciences Publication (BEIESP)

Fig. 9. (a) TG and (b) DTA-Thermograms of hydrated GL30, GL30R5, GL30R7.5 and GL30R10 at 90 days

Published By:
Blue Eyes Intelligence Engineering
and Sciences Publication (BEIESP)